

## Directed Hydroxylation of $sp^2$ and $sp^3$ C–H Bonds Using Stoichiometric Amounts of Cu and $H_2O_2$

Rachel Trammell,<sup>†</sup> Lorenzo D'Amore,<sup>‡</sup> Alexandra Cordova,<sup>†</sup> Pavel Polunin,<sup>†</sup> Nan Xie,<sup>†</sup> Maxime A. Siegler,<sup>||</sup> Paola Belanzoni,<sup>⊥,‡</sup> Marcel Swart,<sup>\*,‡,§</sup> and Isaac Garcia-Bosch<sup>\*,†</sup>

<sup>†</sup>Department of Chemistry, Southern Methodist University, Dallas, Texas 75275, United States

<sup>‡</sup>University of Girona, Campus Montilivi (Ciències), IQCC, 17004 Girona, Spain

<sup>§</sup>ICREA, Pg. Lluís Companys 23, 08010 Barcelona, Spain

<sup>||</sup>Johns Hopkins University, Baltimore, Maryland 21218, United States

<sup>⊥</sup>Dipartimento di Chimica, Biologia e Biotecnologie, Università degli Studi di Perugia, Via Elce di Sotto 8, 06123 Perugia, Italy

<sup>#</sup>Consortium for Computational Molecular and Materials Sciences (CMS)<sup>2</sup>, Via Elce di Sotto 8, 06123 Perugia, Italy

### Supporting Information

**ABSTRACT:** The use of copper for C–H bond functionalization, compared to other metals, is relatively unexplored. Herein, we report a synthetic protocol for the regioselective hydroxylation of  $sp^2$  and  $sp^3$  C–H bonds using a directing group, stoichiometric amounts of Cu and  $H_2O_2$ . A wide array of aromatic ketones and aldehydes are oxidized in the carbonyl  $\gamma$ -position with remarkable yields. We also expanded this methodology to hydroxylate the  $\beta$ -position of alkylic ketones. Spectroscopic characterization, kinetics, and density functional theory calculations point toward the involvement of a mononuclear  $LCu^{II}(OOH)$  species, which oxidizes the aromatic  $sp^2$  C–H bonds via a concerted heterolytic O–O bond cleavage with concomitant electrophilic attack on the arene system.

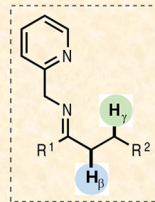
Cu/ $H_2O_2$

#### Recipe #220818: Cu-Directed Hydroxylation

1 equiv. Copper  
1 equiv. Substrate-ligand  
5 equiv.  $H_2O_2$

Note it only takes 30 min!

Measure equal parts of substrate-ligand and Cu. Dissolve and mix in 4 mL of acetone and then add the oxidant. Once mixed, leave at room temperature until either  $H_\beta$  or  $H_\gamma$  is oxidized (Note: the site of hydroxylation depends on the substrate).



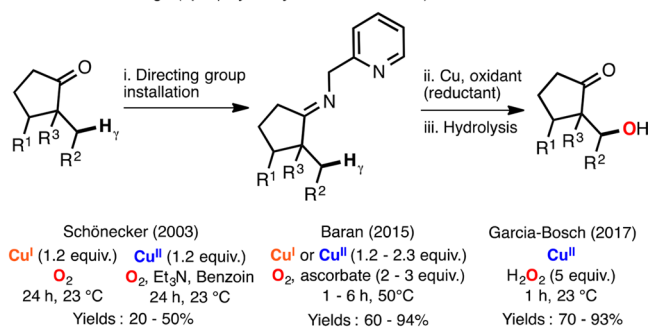
## 1. INTRODUCTION

Synthetic methods that use 3d metals to carry out regioselective C–H hydroxylations are scarce.<sup>1</sup> One of the main challenges of this approach is to overcome the tendency of these metals to generate radical species, which usually lead to unselective C–H oxidations and functional group degradation.<sup>2</sup> Metalloenzymes have evolved to bypass these issues by developing active centers that can regulate the redox reactivity of the metal– $O_2$  intermediates and to control the substrate spatial orientation for site selectivity.<sup>3,4</sup> Que, Costas, and White have shown that non-heme Fe complexes catalyze the regioselective hydroxylation of complex organic molecules with  $H_2O_2$  via formation of Fe–oxo intermediates.<sup>5–7</sup> On the other hand, our research group has recently reported that analogous Cu catalysts react with  $H_2O_2$  to generate unselective hydroxyl radicals (Fenton-like chemistry).<sup>8</sup> The use of directing groups (DGs) is an elegant method for circumventing regioselectivity issues in organic synthesis.<sup>9</sup> We have recently studied the mechanism by which Cu promotes the intramolecular  $\gamma$   $sp^3$  C–H hydroxylation of steroidal iminopyridine substrates,<sup>10</sup> a reaction first developed by Schönecker<sup>11–13</sup> and later optimized by Baran<sup>14</sup> (Figure 1A). On the basis of our findings, we were able to redesign the reaction conditions to use cheaper reagents with shorter reaction times under milder conditions.<sup>10</sup> In this work, we take advantage of

this knowledge to carry out the functionalization of a wide array of substrates containing  $sp^2$  and  $sp^3$  C–H bonds (Figure 1B).

*o*-Acylphenols are commonly found in several bioactive natural products and drugs and are widely used as building blocks in the synthesis of pharmaceuticals and oxygen-containing heterocycles.<sup>15</sup> A classic approach for the synthesis of *o*-acylphenols is a two-step procedure that entails acylation of the phenols followed by Fries rearrangement<sup>16</sup> however, this method is not selective, and the substrate scope is limited.<sup>16</sup> A very attractive synthetic route is the direct regioselective hydroxylation of arylketones. Catalytic amounts of precious metals (Pd, Rh, and Ru) have been used for this purpose, but their reactivity often relies on harsh reaction conditions and the use of expensive hypervalent iodine oxidants [i.e.,  $PhI(CF_3CO_2)_3$ ].<sup>17–19</sup> The Yu research lab showed that Cu can promote intramolecular *ortho* hydroxylation of phenylamides at high temperatures by using excess amounts of a metal source and adding external oxazoline ligands and various additives.<sup>19</sup> Very recently, Uchiyama reported the directed *ortho* hydroxylation of *N,N*-diisopropylamides by deprotonation using excess amounts of a cuprate base followed by

Received: March 28, 2019

A. Previous findings ( $sp^3$   $\gamma$ -hydroxylation of steroids)

## B. This work

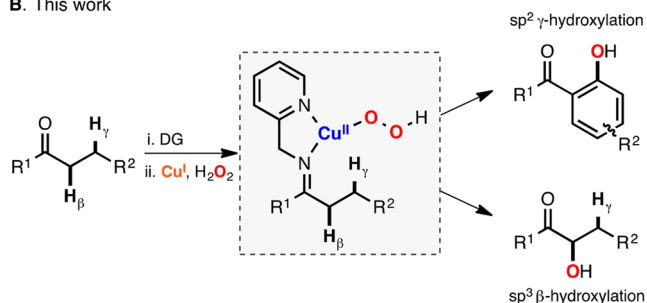


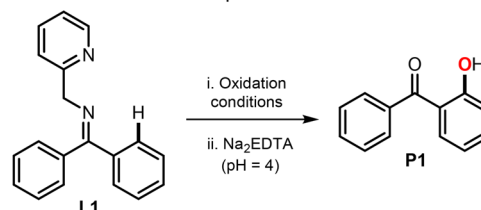
**Figure 1.** Cu-directed hydroxylation of  $sp^2$  and  $sp^3$  C–H bonds.

oxidation with  $tBuOOH$ .<sup>20</sup> Inspired by our findings on Cu-directed hydroxylation of  $sp^3$  C–H bonds using  $H_2O_2$  as an oxidant (see Figure 1A), we decided to determine if a similar methodology could be used for the synthesis of *o*-acylphenols under mild conditions.

The study of the oxidative properties of  $LCu/O_2$  species has led to a better understanding of the reactivity of Cu-dependent monooxygenase enzymes.<sup>21–24</sup> For several examples, the formation of a metastable  $LCu/O_2$  intermediate is followed by the intramolecular oxidation of the ligand scaffold, including ligand hydroxylation,<sup>25,26</sup> sulfoxidation,<sup>27</sup> and N-dealkylation.<sup>28</sup> In selected examples, Cu complexes have been used to promote the intermolecular oxidation of external substrates,<sup>29</sup> with a focus on mimicking the tyrosinase-like *ortho* hydroxylation of phenolates, including stoichiometric<sup>30–32</sup> and catalytic transformations.<sup>33,34</sup> Despite the rich reactivity of Cu/ $O_2$  species in the synthetic inorganic literature, their use in synthetic organic chemistry has been restricted to a handful of examples.<sup>23</sup> Among these, it is worth mentioning Lumb's reports on Cu-catalyzed aerobic functionalization of phenols.<sup>35–37</sup> Réglér pioneered the field of Cu-directed oxidation of C–H bonds,<sup>38,39</sup> an approach that inspired the work of Schönecker<sup>11–13</sup> on steroid  $sp^3$  hydroxylation. Using a similar methodology, Schindler has also shown that bidentate amines can direct the hydroxylation of  $sp^2$  and  $sp^3$  C–H bonds employing  $Cu^I$  and  $O_2$  with modest oxidation yields (<50%).<sup>40</sup> On the basis of these precedents, we report the Cu-directed hydroxylation of  $sp^2$  and  $sp^3$  C–H bonds in which unprecedented regioselectivity and a deeper mechanistic understanding of the reaction mechanism are achieved (Figure 1B).

## 2. RESULTS AND DISCUSSION

**2.1. Synthesis and Oxidation of Imino-Pyridine Substrates.** Condensation of benzophenone, **S1**, with 2-picolylamine led to the formation of the substrate–ligand system **L1** (Figure 2A; see also the Supporting Information for

A. Optimization of Cu oxidation protocol<sup>a</sup>

Entry	Metal source <sup>b</sup>	Oxidant <sup>c</sup>	Solvent	Yield <b>P1</b> (%) <sup>d</sup>
1	$[Cu^I(CH_3CN)_4]PF_6$	$H_2O_2$ (1.5 equiv.)	acetone	65
2	$[Cu^I(CH_3CN)_4]PF_6$	$H_2O_2$ (2.5 equiv.)	acetone	78
3	$[Cu^I(CH_3CN)_4]PF_6$	$H_2O_2$ (5 equiv.)	acetone	85
4	$[Cu^I(CH_3CN)_4]PF_6$	$H_2O_2$ (10 equiv.)	acetone	80
5	$[Cu^I(CH_3CN)_4]PF_6$	$O_2$ , –20 °C	acetone	7
6	$[Cu^I(CH_3CN)_4]PF_6$	$O_2$ , 0 °C	acetone	8
7	$[Cu^I(CH_3CN)_4]PF_6$	$O_2$ , 20 °C	acetone	12
8	$[Cu^I(CH_3CN)_4]PF_6$	$O_2$ , 50 °C	acetone	46
9	$[Cu^I(CH_3CN)_4]PF_6$	$H_2O_2$	$CH_3CN$	44
10	$[Cu^I(CH_3CN)_4]PF_6$	$H_2O_2$	THF	66
11	$[Cu^I(CH_3CN)_4]PF_6$	$H_2O_2$	$CH_2Cl_2$	49
12	$[Cu^I(CH_3CN)_4]PF_6$	$tBuOOH$	acetone	0
13	$[Cu^I(CH_3CN)_4]PF_6$	CumOOH	acetone	0
14	$Cu^I(OAc)$	$H_2O_2$	acetone	0
15	$[Cu^I(CH_3CN)_4](CF_3SO_3)$	$H_2O_2$	acetone	76
16	$Cu^II(CF_3SO_3)_2$	$H_2O_2$	acetone	45
17	$Cu^IICl_2$	$H_2O_2$	acetone	6
18	$Cu^II(OAc)_2$	$H_2O_2$	acetone	0
19	$Ni^II(CF_3SO_3)_2$	$H_2O_2$	acetone	0
20	$Fe^II(CF_3SO_3)_2$	$H_2O_2$	acetone	0
21	$Mn^II(CF_3SO_3)_2$	$H_2O_2$	acetone	0
22	$[Cu^I(CH_3CN)_4]PF_6$	$H_2O_2$	acetone	70 <sup>e</sup>
23	$Cu^II(NO_3)_2 \cdot 3H_2O$	$H_2O_2$	acetone	22
24	$Cu^II(NO_3)_2 \cdot 3H_2O$	$H_2O_2$	THF	37
25	$Cu^II(NO_3)_2 \cdot 3H_2O$	$H_2O_2/OH^-$	acetone	80 <sup>f</sup>

<sup>a</sup> All reactions were performed with  $[L1] = 40$  mM. <sup>b</sup> 1 equiv. <sup>c</sup> 5 equiv. of 30%  $H_2O_2$  (aq.) were used unless stated (30 min, r.t.). <sup>d</sup> Yields were determined by  $^1H$ -NMR using 1,3,5-trimethoxybenzene as internal standard. <sup>e</sup> Oxidation of isolated  $[(L1)Cu^I(CH_3CN)](PF_6)$ . <sup>f</sup> 1 equiv. of  $NMe_4OH \cdot 5H_2O$

## B. Gram scale hydroxylation of benzophenone

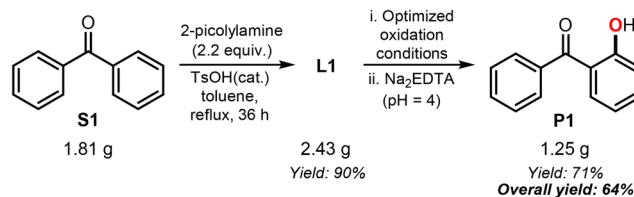


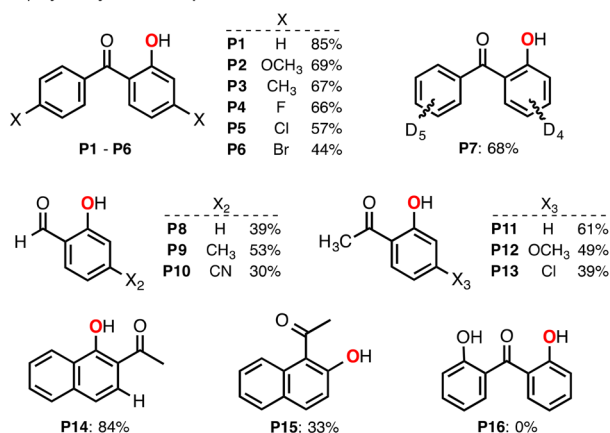
**Figure 2.** (A) Optimization of the reaction conditions for the hydroxylation of **L1**. (B) Gram scale oxidation of **S1** using the optimized  $Cu^I/H_2O_2$  conditions. See the Supporting Information.

experimental details). The Cu-promoted oxidation of **L1** was optimized under various reaction conditions (Figure 2A). One-pot mixing of equimolar amounts of **L1** and  $[Cu^I(CH_3CN)_4](PF_6)$  in acetone followed by addition of 5 equiv of  $H_2O_2$  produced the hydroxylation product **P1** in excellent yields (Figure 2A, entry 3). The use of various Cu sources was tested (Figure 2A, entries 14–18) with  $[Cu^I(CH_3CN)_4](PF_6)$  reaching the highest yields ( $\leq 85\%$ ). Acetone was found to be the best solvent, followed by THF,  $CH_2Cl_2$ , and  $CH_3CN$  (Figure 2A, entries 3 and 9–11). We also analyzed the use of  $O_2$  as an oxidant. We observed that an increase in the reaction temperature from –20 to 50 °C (Figure 2A, entries 5–8) afforded higher yields (from 7% to 46%). A similar effect was observed in the oxidation of  $sp^3$  steroidal systems and was attributed to the formation of  $H_2O_2$  via reduction of  $O_2$  by  $Cu^I$  (i.e., formation of  $Cu^{II}$  and superoxide) and subsequent oxidation of the solvent, which is favored at high temperatures.<sup>10</sup> The efficiency of other oxidants such as cumyl

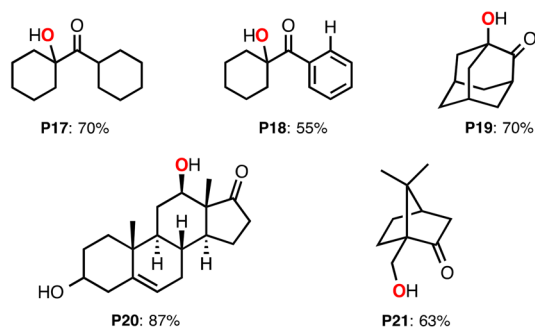
hydroperoxide (CumOOH) and *tert*-butyl hydroperoxide (BuOOH) was also studied (Figure 2A, entries 12 and 13, respectively), but only H<sub>2</sub>O<sub>2</sub> produced the oxidation product P1. Noticeably, when other first-row transition metal sources were used (e.g., Mn<sup>II</sup>, Fe<sup>II</sup>, and Ni<sup>II</sup>), P1 was not formed and only starting material was recovered (Figure 2A, entries 19–21). We performed the oxidation of L1 on a gram scale using the optimized conditions (1 equiv of Cu<sup>I</sup> and 5 equiv of H<sub>2</sub>O<sub>2</sub>), which afforded the hydroxylation product, P1, in 71% yield (Figure 2B; note that a 64% overall yield includes the installation of the directing group).

With the most suitable oxidation conditions in hand, we explored the hydroxylation of the substrate–ligand systems derived from the condensation of 2-picolylamine with various benzophenones, acetophenones, and benzaldehydes (Figure 3A). For all of these systems, we obtained the oxidation products derived from the  $\gamma$ -hydroxylation of the sp<sup>2</sup> C–H bond (P1–P13) with moderate to excellent yields (30–85%). Substrates in which the oxidation can occur at multiple sites

#### A. $\gamma$ -hydroxylation of sp<sup>2</sup> C–H bonds



#### B. $\beta$ and $\gamma$ -hydroxylation of sp<sup>3</sup> C–H bonds



#### C. Divergent regioselectivity in Cu-promoted hydroxylations

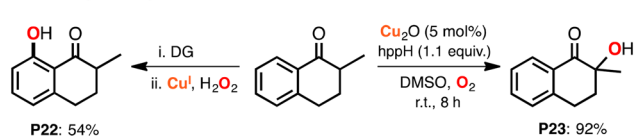


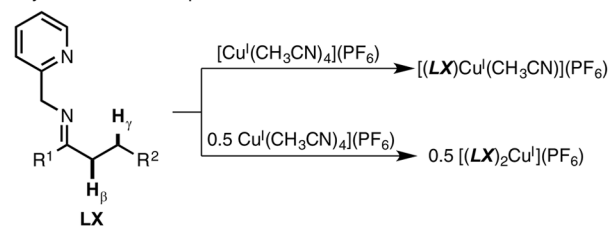
**Figure 3.** (A)  $\gamma$ -Hydroxylation of sp<sup>2</sup> C–H bonds. (B)  $\beta$ - and  $\gamma$ -hydroxylation of sp<sup>3</sup> C–H. (C) Divergent regioselectivity:  $\gamma$ -sp<sup>2</sup> hydroxylation described this work (DG, 2-picolylamine) vs  $\beta$ -sp<sup>3</sup> hydroxylation reported by Schoenebeck.<sup>42</sup> All reactions were performed with 40 mM LX using 5 equiv of 30% H<sub>2</sub>O<sub>2</sub> (2.5 equiv for sp<sup>2</sup> C–H hydroxylation) for 30 min at room temperature in acetone. See the Supporting Information for further details.

(e.g., 2-acetonaphthone can be oxidized at the  $\beta$  sp<sup>3</sup> position or two different  $\gamma$  sp<sup>2</sup> positions) were also tested. Oxidation of 2-acetonaphthone occurred selectively at position 1 of the naphthyl ring with remarkable yields (P14, 84%). Similarly, the oxidation of the imino-pyridine substrate derived from 1-acetonaphthone led to the sp<sup>2</sup> hydroxylation product (P15, 33%). We also aimed to verify that our oxidation conditions did not generate overoxidation products. To do so, we synthesized the imino-pyridine system derived from P1 and subjected it to oxidation with Cu<sup>I</sup> and H<sub>2</sub>O<sub>2</sub>, which led to recovery of P1 (P16, 0%) and differed from other Cu/O<sub>2</sub> systems in which intramolecular hydroxylation of phenol substituents was observed.<sup>41</sup>

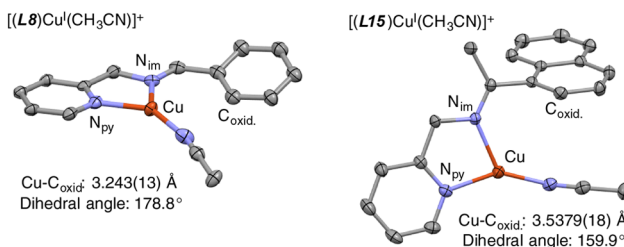
A new set of sp<sup>3</sup> C–H bond-containing systems were also oxidized using Cu<sup>I</sup> and H<sub>2</sub>O<sub>2</sub> (Figure 3B). The substrate–ligand system derived from dicyclohexyl ketone was selectively oxidized at the  $\beta$  position in high yields (P17, 70%). This selectivity differs from previous findings in which the sp<sup>3</sup> C–H hydroxylation occurred at the  $\gamma$  position. Like in previous reports, the systems derived from dehydro-*epi*-androsterone and *R*-camphor were selectively oxidized at the  $\gamma$  site (P20 and P21).<sup>10–14</sup> The  $\beta$  selectivity was also observed by the oxidation of the asymmetric system derived from cyclohexyl phenyl ketone (P18, 55%). More importantly, our methodology allowed synthesis of the  $\beta$ -hydroxylation product of 2-adamantanone with remarkable yields (P19, 70%), which is inaccessible using classic silyl enol ether/peroxyacid oxidations and other base-triggered oxidation reactions.<sup>42–45</sup> Our methodology also resulted in the  $\gamma$  sp<sup>2</sup> hydroxylation of cyclic ketones such as 2-methyl-1-tetralone with good yields (Figure 3C, P22, 54%). Interestingly, this regioselectivity differs from the reactivity observed by Schoenebeck and co-workers, in which a combination of Cu<sub>2</sub>O, a strong base, and O<sub>2</sub> led to the oxidation of the  $\beta$ -sp<sup>3</sup> C–H bond (P23, 92%).<sup>42</sup>

**2.2. Synthesis of Copper Complexes.** With the substrate–ligand systems in hand, we synthesized and characterized cuprous complexes in which one or two ligand scaffolds are bound to the metal ion (Figure 4A; see also the

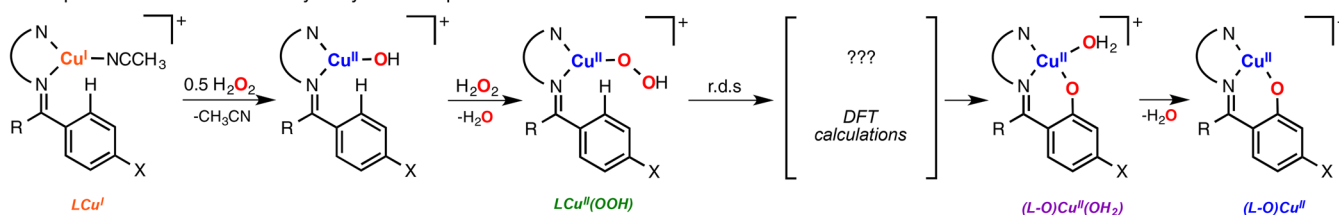
#### A. Synthesis of Cu complexes



#### B. X-ray diffraction analysis

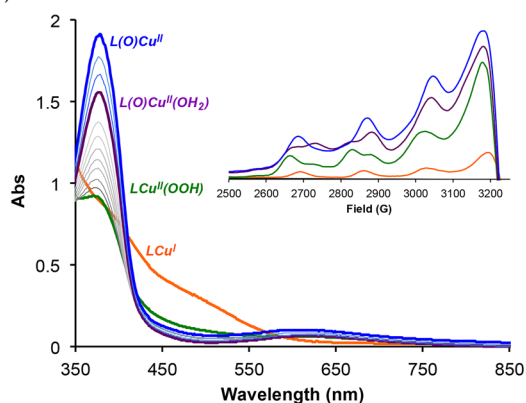


**Figure 4.** (A) Synthesis of Cu<sup>I</sup> substrate–ligand complexes. (B) X-ray diffraction analyses of the systems derived from benzaldehyde (left) and 1-acetophenone (right). See the Supporting Information for further details.

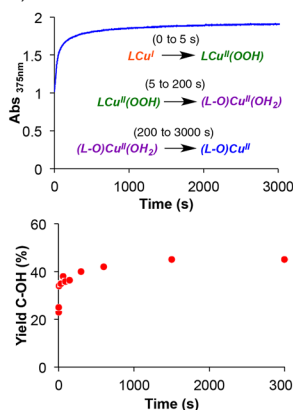
A. Proposed mechanism for the hydroxylation of  $sp^2$  C-H bonds

## B. Spectroscopic and kinetic analysis

## i) UV-vis and EPR



## ii) UV-vis vs. Yield



## iii) Kinetics

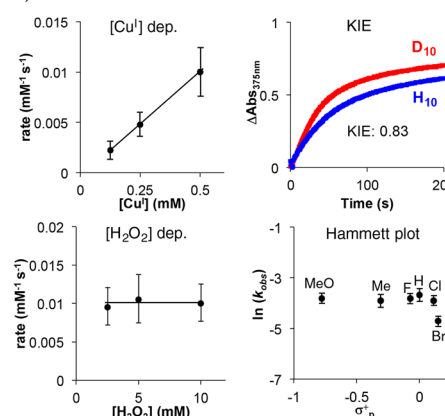


**Figure 5.** (A) Proposed reaction mechanism for the Cu-directed  $sp^2$  C–H hydroxylation with  $H_2O_2$ . (B) (i) UV–vis and EPR characterization of the reaction intermediates formed upon addition of  $H_2O_2$  (20 equiv) to the  $[(LI)Cu^I(CH_3CN)]^+$  complex (0.5 mM) in acetone at  $-20^\circ C$  (note that the EPR shows mixtures of intermediates and only the main contributor is indicated; the  $g_{\perp}$ ,  $g_{\parallel}$ , and  $A_{\parallel}$  values can be found in the Supporting Information; also see the Supporting Information for  $Cu^{II}$  signal quantification). (ii) Evolution of the absorbance at 380 nm of the reaction (top) and analysis of the hydroxylation yields over time (bottom). (iii) Kinetic analysis of the reaction by varying  $[Cu^I]_0$  and  $[H_2O_2]_0$ , KIE analysis, and a Hammett plot (see the text and Supporting Information for details).

Supporting Information). X-ray diffraction analysis of the isolated substrate–ligand Cu complexes provided structural information about the site of hydroxylation (Figure 4B; see also the Supporting Information). For example, analysis of the  $Cu^I$  system derived from 2-acetophenone (L15) showed that the  $\gamma$   $sp^2$  C–H position that will undergo oxidation ( $C_{oxid.}$ ) is the closest to the Cu ion, with the  $CH_3$  site pointed away from the  $CuN_3$  T-shaped core.

**2.3. Mechanistic Studies.** With the isolated complexes  $[(LX)Cu^I(CH_3CN)]^+$ , we studied the mechanism by which the Cu-directed  $sp^2$  hydroxylation takes place (Figure 5). In our previous study, we proposed that the reaction between  $LCu^I$  and  $O_2$  generated  $LCu^{II}$  and superoxide that, upon oxidation of the solvent, formed  $H_2O_2$ .<sup>10</sup> Subsequent reaction of  $LCu^{II}$  and  $H_2O_2$  would produce a mononuclear  $LCu^{II}(OOH)$  intermediate before the rate-determining step (r.d.s.). We found that the same  $LCu^{II}(OOH)$  species could also be formed by addition of  $H_2O_2$  to the  $LCu^I$  or  $LCu^{II}$  complexes.<sup>46</sup> For the benzophenone-derived  $Cu^I$  complexes described herein, we suggest a similar hydroxylation pathway (Figure 5A). The reaction between  $LCu^I$  and  $H_2O_2$  was followed by ultraviolet visible (UV–vis) and electron paramagnetic resonance (EPR) (Figure 5B, i). Addition of  $H_2O_2$  (20 equiv) to a 0.5 mM acetone solution of  $[(LI)Cu^I(CH_3CN)]^+$  at  $-20^\circ C$  (orange spectrum) generated a species with spectral features characteristic of  $LCu^{II}(OOH)$  complexes (green spectrum,  $\lambda_{max} = 380–400$  nm,  $\epsilon = 2000 M^{-1} cm^{-1}$ ).<sup>46</sup> Decomposition of the metastable  $LCu^{II}(OOH)$  produced two mononuclear  $Cu^{II}$  species in a stepwise manner ( $\lambda_{max} \sim 380$  nm), which we assign as  $Cu^{II}$  compounds in which the  $\gamma$   $sp^2$  C–H bond has been oxidized (purple and blue

spectra in Figure 5B, i). We independently synthesized and characterized the  $Cu^{II}$ -bound hydroxylation product (ligand derived from P1), and its UV–vis spectrum overlaps with the species formed in the  $LCu^I/H_2O_2$  reaction (see the Supporting Information). Fitting of the absorbance at 380 nm (Figure 5B, ii, top) suggested a three-step reaction in which the initial  $LCu^I$  is quickly transformed to the  $LCu^{II}(OOH)$  complex (0–5 s), which evolves to generate two forms of the hydroxylation product  $[(L-O)Cu^{II}(OH_2)]$  from 5 to 200 s and  $(L-O)Cu^{II}$  from 200 to 3000 s]. The same species are observed by EPR, during which, upon addition of  $H_2O_2$  to  $LCu^I$ , three distinctive mononuclear  $Cu^{II}$  complexes are consecutively formed (Figure 5B, i, inset). We confirmed that the hydroxylation of the substrate occurred at short reaction times (from 5 to 200 s after addition of  $H_2O_2$ ) by analyzing the hydroxylation yields at different reaction times (Figure 5B, ii, bottom).

Kinetic analysis at different Cu and  $H_2O_2$  concentrations indicated that the hydroxylation rate is first-order in  $[LCu^I]_0$  and zero-order in  $[H_2O_2]_0$ , which suggested that the intramolecular hydroxylation is not a one-step bimolecular process between  $LCu^I$  and  $H_2O_2$  and that the decay of the putative  $LCu^{II}(OOH)$  intermediate occurs in the r.d.s. (Figure 5B, iii). The kinetic isotope effect (KIE) of the reaction was obtained by comparing the reaction rates of the benzophenone-derived ligand system L1 with the benzophenone- $d_{10}$  analogue L7 (Figure 5B, iii; see also the Supporting Information). The KIE value ( $\sim 0.83$ ) indicates that during the r.d.s. the C–H bond that is oxidized undergoes  $sp^2$  to  $sp^3$  hybridization, which is consistent with an electrophilic attack of the  $LCu^{II}(OOH)$  on the arene substrate.<sup>47</sup>

We also obtained the reaction rates of  $\text{Cu}^{\text{I}}$  substrate–ligand systems derived from 4-substituted benzophenones ( $X = \text{MeO}$ ,  $\text{Me}$ ,  $\text{F}$ ,  $\text{Cl}$ , or  $\text{Br}$ ). The hydroxylation rates were found to be independent of the substituent ( $k_{\text{obs}}$  vs  $\sigma^+_{\text{p}}$ , Hammett plot, in Figure 5B, iii), which might appear to contradict the proposed direct electrophilic attack of the  $\text{LCu}^{\text{II}}(\text{OOH})$  on the aromatic system, because this reaction would be accelerated for electron-donating systems.<sup>48</sup> However, the possibility that the introduction of electron-donating or electron-withdrawing substituents into the substrate–ligand structure might also affect the electrophilicity of the  $\text{LCu}^{\text{II}}(\text{OOH})$  cores should be considered: for example, the use of the 4-MeO substituent will produce a substrate more reactive toward electrophilic attack but will also lead to a more electron-rich  $\text{LCu}^{\text{II}}(\text{OOH})$  species, and hence less electrophilic (see Figure 6B), compensating for the substrate substituent effect.

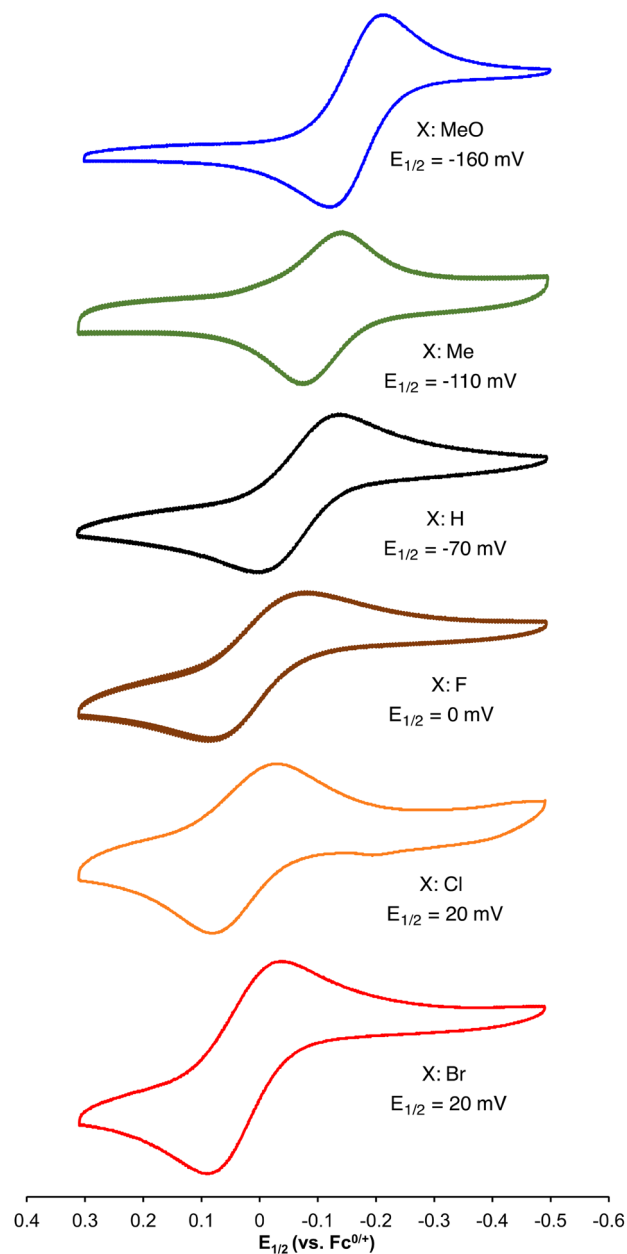
To substantiate this mechanistic hypothesis, we measured the redox potentials of the benzophenone-derived Cu complexes (Figure 6). We found that the complex derived from benzophenone [ $(\text{L1})\text{Cu}^{\text{I}}(\text{CH}_3\text{CN})$ ]<sup>+</sup> was reversibly oxidized in  $\text{CH}_3\text{CN}$  at  $-0.07$  V versus ferrocene/ferrocenium ( $\text{Fc}^{0/+}$ ). For the systems containing electron-donating groups, the  $\text{Cu}^{\text{I}}/\text{Cu}^{\text{II}}$  redox couple shifted to lower redox potentials ( $-0.11$  V for 4-Me and  $-0.16$  V for 4-MeO), while for the systems with electron-withdrawing substituents, the redox potentials were found at higher potentials ( $0.00$  V for 4-F and  $0.02$  V for 4-Cl and 4-Br).

Overall, substitution of position 4 of the substrate–ligand phenyl substituent led to a change in the redox potentials of almost 0.2 V, with the 4-MeO system having the lowest redox potential and the 4-Br system having the highest, which we believe corroborates our hypothesis about the electrophilicity of the putative  $\text{LCu}^{\text{II}}(\text{OOH})$  reactive intermediates [i.e., 4-MeO substrate more prone to electrophilic attack but  $\text{LCu}^{\text{II}}(\text{OOH})$  less electrophilic].

**2.4. Computational Studies.** Density functional theory (DFT) calculations were carried out to improve our understanding of the mechanism by which the putative mononuclear  $\text{LCu}^{\text{II}}(\text{OOH})$  promotes intramolecular hydroxylation (Figure 7). Our calculations (including solvent and scalar relativistic corrections) at S12g/TZ2P//BP86-D3/TDZP showed that the end-on  $\text{Cu}^{\text{II}}$ –hydroperoxide intermediate (RC) undergoes heterolytic O–O cleavage with concomitant electrophilic attack of the phenyl substituent.<sup>49</sup> We found that the resulting Wheland-like intermediate<sup>50</sup> (INT1) isomerized to a Cu complex in which the H at the  $\gamma$ -carbon is transferred to the  $\delta$  aromatic position (INT2).<sup>51</sup> This hydrogen shift could then trigger the deprotonation of the organic fragment by the  $\text{Cu}^{\text{II}}$ –OH core (TS3) to generate  $\text{H}_2\text{O}$  and recover the aromaticity of the ring (PC).

On the basis of these results, O–O bond cleavage is the reaction step that requires more energy. This agrees with our kinetic measurements [i.e., first-order dependence of  $[\text{Cu}]_0$ , zero-order dependence of  $[\text{H}_2\text{O}_2]_0$ , and KIE (*vide supra*)] and spectroscopic characterizations, all of which suggested that the O–O bond cleavage, coupled with electrophilic attack, is rate-limiting. We also carried out the same calculations for the 4-substituted systems 4-MeO and 4-Br. We computed that the energetics of the rate-determining step for 4-MeO and 4-Br were very similar to the values found for the 4-H system (15.8 kcal/mol for 4-H, 16.2 kcal/mol for 4-MeO, and 14.6 kcal/mol for 4-Br). These findings ( $\sim 1$  kcal/mol difference between the 4-substituted systems) are in agreement with the kinetic data

A. Cyclic voltammetry of  $[(\text{LX})\text{Cu}^{\text{I}}(\text{CH}_3\text{CN})]^+$  complexes.



B. Analysis of the electronic effects on the reactivity of  $\text{Cu}^{\text{II}}\text{OOH}$  cores

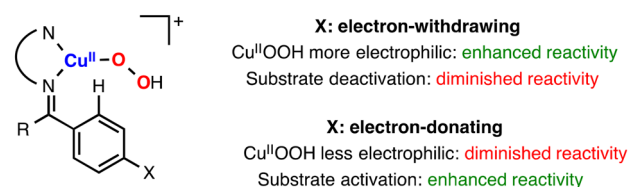
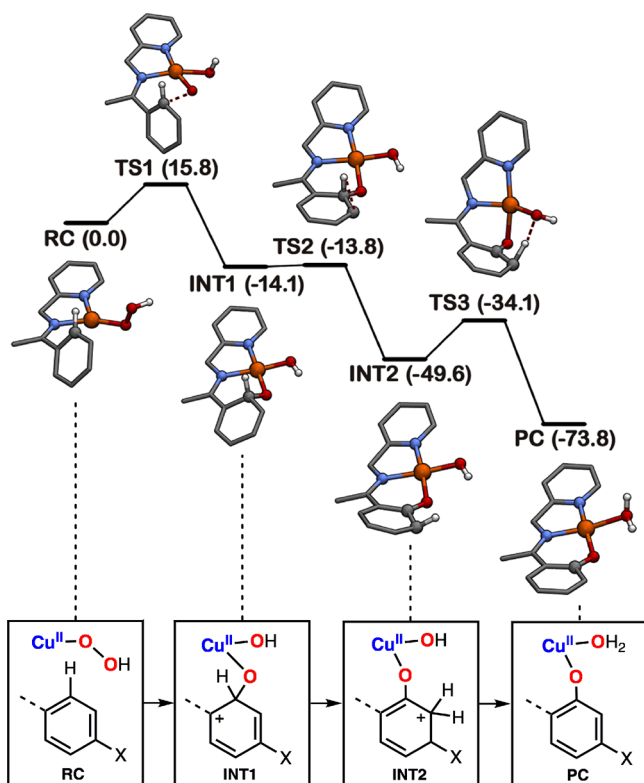


Figure 6. (A) Cyclic voltammetry measurements for the family of benzophenone-derived  $\text{Cu}^{\text{I}}$  complexes. (B) Effects on the reactivity of the putative  $\text{LCu}^{\text{II}}(\text{OOH})$  species.

described above in which similar reaction rates were observed for all of the 4-substituted benzophenone–ligand complexes.

**2.5. Mechanistic Considerations.** Copper(I) complexes react with  $\text{O}_2$  to generate fleeting mononuclear  $\text{Cu}/\text{O}_2$  species that are difficult to trap due to their tendency to react with other  $\text{LCu}^{\text{I}}$  equivalents and form more stable  $\text{Cu}_2\text{O}_2$  cores.<sup>21,52</sup>



**Figure 7.** DFT calculations on the Cu-directed hydroxylation of  $sp^2$  C–H bonds.

Because of this, the reactivity of  $Cu_2O_2$  species has been studied in detail, and it has been established that end-on dicopper(II)–peroxide intermediates are normally nucleophilic oxidants while side-on dicopper(II)–peroxide complexes and dicopper(III) bis- $\mu$ -oxo compounds are considered electrophilic oxidants.<sup>32,53,54</sup> On the other hand, mononuclear Cu/O<sub>2</sub> complexes are scarce and the study of their reactivity has been restricted to a few selected systems.<sup>55–58</sup>

Several research groups have reported that both mononuclear and dinuclear Cu/O<sub>2</sub> species can perform intramolecular C–H hydroxylations (Figure 8A). For example, Karlin and co-workers observed that a Cu complex bearing a superbasic tetradentate ligand (Figure 8A, i) could undergo intramolecular  $sp^3$  C–H hydroxylation via formation of a putative mononuclear  $LCu^{II}$ –oxyl species.<sup>25</sup> The same research group also found that an  $LCu^{II}$ (OOH) complex promoted the intramolecular  $sp^2$  hydroxylation of a tmpa-derived tetradentate scaffold and showed that the corresponding  $L_2Cu_2O_2$  adduct did not undergo intramolecular ligand oxidation (Figure 8A, ii).<sup>59</sup> Itoh and co-workers were able to generate and characterize a unique  $Cu^{II}$ –superoxide complex that underwent intramolecular C–H hydroxylation via H atom abstraction of the supporting tridentate ligand (Figure 8A, iii).<sup>26,60</sup> Réglie, Schindler,<sup>40,61</sup> and Tolman<sup>48</sup> have reported that for some bidentate and tridentate ligands, these intramolecular hydroxylations entail the formation of  $Cu_2O_2$  cores because N2 and N3 scaffolds usually favor their formation<sup>52</sup> [note that both Schindler and Tolman observed the formation of  $L_2Cu^{III}_2(O^{2-})_2$  cores before ligand hydroxylation]. On the basis of reaction yields, a similar mechanistic scenario was hypothesized by Schönecker and co-workers for the intramolecular hydroxylation of  $sp^3$  C–H bonds in steroid-derived bidentate ligands.<sup>11–13</sup> However, we have recently proposed

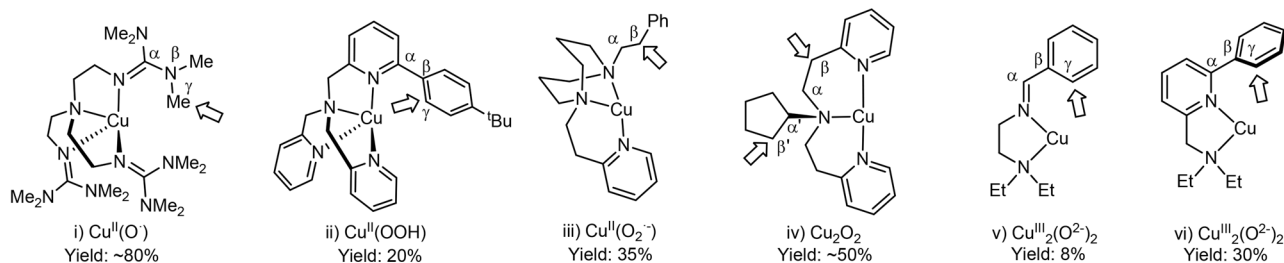
that these ligand scaffolds are more likely oxidized via formation of mononuclear Cu/O<sub>2</sub> intermediates (Figure 8B).<sup>10</sup>

Our mechanistic findings supported the idea that  $H_2O_2$  is the active oxidant in these intramolecular hydroxylations.<sup>10</sup> We proposed that the reaction between  $LCu^I$  and  $O_2$  generated  $LCu^{II}$  and free superoxide, which was reduced to  $H_2O_2$  via solvent oxidation. The resulting  $LCu^{II}$  would then react with  $H_2O_2$  to produce a mononuclear  $LCu^{II}$ (OOH) intermediate before ligand hydroxylation. We found that this  $LCu^{II}$ (OOH) species could also be generated by adding  $H_2O_2$  to  $LCu^I$ , which would form sequentially  $LCu^{II}$ (OH) and  $LCu^{II}$ (OOH). Alternatively, we observed that the  $LCu^{II}$ (OOH) could also be formed by addition of  $H_2O_2$  to the corresponding  $LCu^{II}$  complex in a presence of a base. On the basis of mechanistic evidence, we suggested that the mononuclear  $LCu^{II}$ (OOH) complex underwent homolytic O–O bond cleavage to generate a hydroxyl radical, which would abstract a H atom from the  $\gamma$   $sp^3$  C–H bond of the ligand scaffold before C–O bond formation (Figure 8B). The mechanistic studies of  $sp^2$  hydroxylation presented herein also support the formation of  $LCu^{II}$ (OOH) intermediates. However, the reaction pathway for  $sp^2$  C–H hydroxylation seems to entail a concerted C–O bond formation with heterolytic O–O bond cleavage as the rate-determining step of the reaction rather than homolytic cleavage.

As we have shown, the  $LCu^{II}$ (OOH) complex is formed by addition of  $H_2O_2$  to the copper(I) complex (see Figure 5B). We also tested if  $LCu^{II}$ (OOH) could be generated by adding  $H_2O_2$  to a solution of  $LCu^{II}$  and  $NMe_4OH$  (see the Supporting Information). Interestingly, we observe that the UV–vis changes and the rate of hydroxylation for **L1** with  $Cu^{II}$ ,  $H_2O_2$ , and hydroxide were identical to those found in the oxidation of **L1** with  $Cu^I$  and  $H_2O_2$  [note that the use of  $NMe_4OH$  also led to higher reaction yields in the oxidation of **L1** with  $Cu^{II}(NO_3)$  (see entry 25 in Figure 2)]. We also carried out the oxidation of **L7** (deuterated version of **L1**) in the presence of  $Cu^{II}$ ,  $H_2O_2$ , and  $HO^-$ , and the rates of hydroxylation were also similar to those calculated in  $Cu^I/H_2O_2$ , leading to an inverse kinetic isotope effect [KIE = 0.89 (see the Supporting Information)]. These findings suggest that under both oxidation conditions ( $Cu^I/H_2O_2$  or  $Cu^{II}/H_2O_2/HO^-$ ) the same reaction intermediates are formed.

It is worth mentioning that the formation of dinuclear  $Cu_2O_2$  species under the reaction conditions presented here cannot be ruled out. However, the fact that the  $Cu^I$  complexes do not generate  $Cu_2O_2$  cores at low temperatures upon reacting with  $O_2$  suggests that these species are not involved in the oxidation of the ligand scaffold. The first-order dependence on  $[LCu^I]_0$  and zero-order dependence on  $[H_2O_2]_0$ , the observed inverse kinetic isotope effect, and the spectroscopic characterization of the reaction intermediates point toward the involvement of a mononuclear species as the active hydroxylating agent. The formation of a  $Cu_2O_2$  species after the rate-determining step and before C–H oxidation would not lead to a kinetic isotope effect (KIE = 1). The generation of a  $Cu_2O_2$  core before the rate-determining step could also show a first-order dependence on  $[LCu^I]_0$  and a zero-order dependence on  $[H_2O_2]_0$ , but if that were the case, the putative  $Cu_2O_2$  species would accumulate before ligand oxidation (i.e.,  $r.d.s.$ ) and would be observed spectroscopically [ $Cu^{II}_2(O_2^{2-})$  and  $Cu^{III}_2(O_2^{2-})$  intermediates are EPR silent, and their UV–vis features are very intense and characteristic]. However, the possible involvement of dinuclear species was computed, and

## A. Selected examples of Cu complexes that undergo intramolecular hydroxylation



## B. Proposed mechanisms for the Cu-directed hydroxylation of C-H bonds

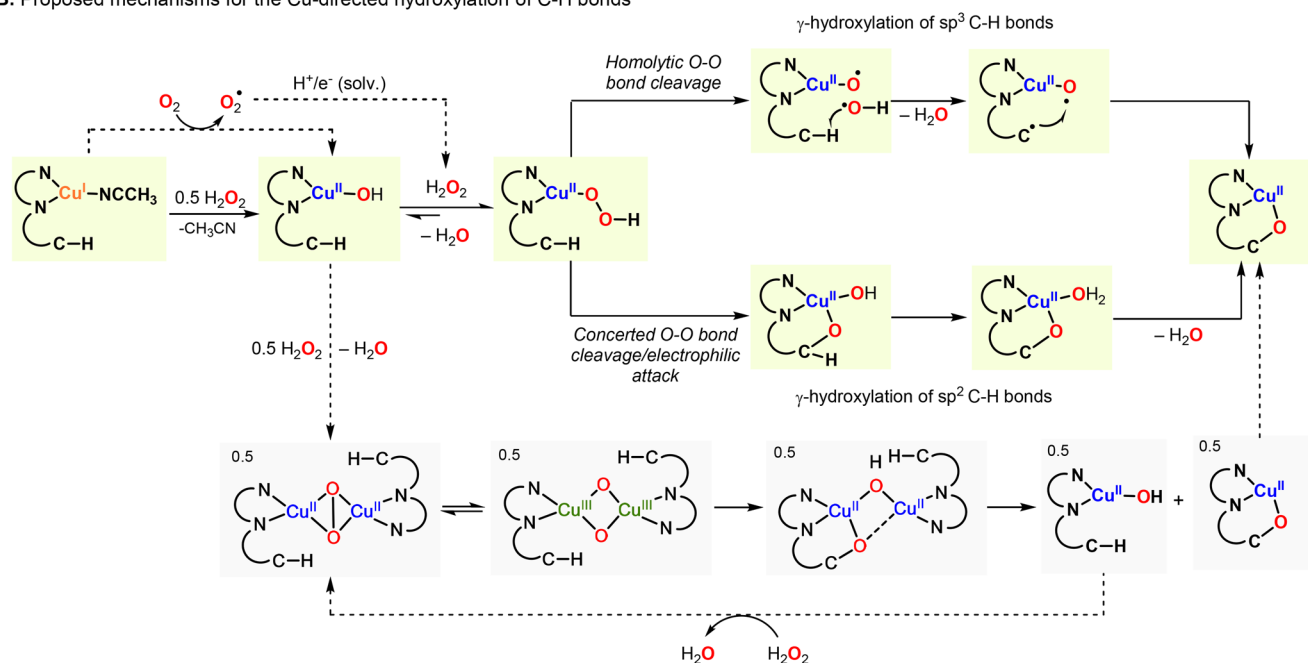


**Figure 8.** (A) Copper complexes that undergo intramolecular C-H hydroxylation via formation of mononuclear or dinuclear Cu/O<sub>2</sub> species. (B) Proposed reaction mechanisms for the intramolecular  $\gamma$ -hydroxylation of C-H bonds discussed herein.

we found that the activation energy for the intramolecular  $\text{sp}^2$  C-H hydroxylation is slightly lower than that found for the  $\text{LCu}^{\text{II}}(\text{OOH})$  intermediate (see the [Supporting Information](#)). Our calculations also indicate that the generation of the  $\text{L}_2\text{Cu}_2\text{O}_2$  cores from  $\text{LCu}^{\text{I}}(\text{OOH})$  is exergonic [ $2\text{LCu}^{\text{I}}(\text{OOH}) \leftrightarrow \text{L}_2\text{Cu}_2^{\text{II}}(\text{O}_2^{2-}) + \text{H}_2\text{O}_2$  ( $\Delta G \sim -7$  kcal/mol)], but the fact the reactions are carried out under excess amounts of  $\text{H}_2\text{O}_2$  might favor the formation of the mononuclear  $\text{LCu}^{\text{II}}(\text{OOH})$  species, a behavior that has also been observed in the Cu-catalyzed hydroxylation of benzene by dicopper species with  $\text{H}_2\text{O}_2$ .<sup>62</sup>

### 3. CONCLUSIONS AND FUTURE PERSPECTIVES

In summary, we report here a synthetic protocol for the functionalization of ketones (and aldehydes) based on the use of directing groups (easily installed and removed), Cu, and  $\text{H}_2\text{O}_2$ , which resulted in hydroxylation products with remarkable yields and unprecedented selectivity (i.e.,  $\beta$ -hydroxylation of  $\text{sp}^3$  systems and selective hydroxylation in unsymmetric ketones). Close examination of the overall reaction mechanism led us to propose an  $\text{LCu}^{\text{II}}(\text{OOH})$  species as a key reaction intermediate, which has also been invoked in some Cu-containing metalloenzymes (e.g., lytic polysaccharide monooxygenases).<sup>63</sup> Inspired by these findings, our lab is now focused on rationally modifying the directing

group to promote the hydroxylation of different substrate sites ( $\beta$  vs  $\gamma$  vs  $\delta$ ) and to generate a wide variety of  $\text{Cu}_n/\text{O}_2$  species (mononuclear and dinuclear) that will lead to a better understanding of the reactivity of Cu-dependent monooxygenases.

## ■ ASSOCIATED CONTENT

### 📄 Supporting Information

The Supporting Information is available free of charge on the ACS Publications website at DOI: [10.1021/acs.inorgchem.9b00901](https://doi.org/10.1021/acs.inorgchem.9b00901).

Experimental details, including substrate–ligand synthesis and oxidation, complex synthesis and characterization, kinetic analysis, spectroscopic characterization, and DFT calculations ([PDF](#)).

### Accession Codes

CCDC 1880982–1880987 contain the supplementary crystallographic data for this paper. These data can be obtained free of charge via [www.ccdc.cam.ac.uk/data\\_request/cif](http://www.ccdc.cam.ac.uk/data_request/cif), or by emailing [data\\_request@ccdc.cam.ac.uk](mailto:data_request@ccdc.cam.ac.uk), or by contacting The Cambridge Crystallographic Data Centre, 12 Union Road, Cambridge CB2 1EZ, UK; fax: +44 1223 336033.

## AUTHOR INFORMATION

## Corresponding Authors

\*E-mail: marcel.swart@udg.edu.

\*E-mail: igarciabosch@smu.edu.

## ORCID

Lorenzo D'Amore: 0000-0003-2245-1956

Paola Belanzoni: 0000-0002-1286-9294

Marcel Swart: 0000-0002-8174-8488

Isaac Garcia-Bosch: 0000-0002-6871-3029

## Notes

The authors declare no competing financial interest.

## ACKNOWLEDGMENTS

The authors thank the Robert A. Welch Foundation, the National Institutes of Health (Grant R15GM128078 to I.G.-B.), MINECO (CTQ2017-87392-P), UdG (IFUdG2016 fellowship to L.D.), and FEDER (UNGI10-4E-801 to M.S.) for financial support, CSUC for extensive computer time, and SMU for financial support and facilities. The authors thank Dr. Vogel and Dr. Wise (SMU) for help with EPR and Dr. Baran for providing ligand systems L20 and L21 and for helpful advice.

## REFERENCES

- (1) Hartwig, J. F. Evolution of C–H Bond Functionalization from Methane to Methodology. *J. Am. Chem. Soc.* **2016**, *138*, 2–24.
- (2) Stavropoulos, P.; Çelenlilgil-Çetin, R.; Tapper, A. E. The Gif Paradox. *Acc. Chem. Res.* **2001**, *34*, 745–752.
- (3) Costas, M. Selective C–H oxidation catalyzed by metalloporphyrins. *Coord. Chem. Rev.* **2011**, *255*, 2912–2932.
- (4) Solomon, E. I.; Heppner, D. E.; Johnston, E. M.; Ginsbach, J. W.; Cirera, J.; Qayyum, M.; Kieber-Emmons, M. T.; Kjaergaard, C. H.; Hadt, R. G.; Tian, L. Copper Active Sites in Biology. *Chem. Rev.* **2014**, *114*, 3659–3853.
- (5) Oloo, W. N.; Que, L. Bioinspired Nonheme Iron Catalysts for C–H and C=C Bond Oxidation: Insights into the Nature of the Metal-Based Oxidants. *Acc. Chem. Res.* **2015**, *48*, 2612–2621.
- (6) Gómez, L.; Garcia-Bosch, I.; Company, A.; Benet-Buchholz, J.; Polo, A.; Sala, X.; Ribas, X.; Costas, M. Stereospecific C–H Oxidation with H<sub>2</sub>O<sub>2</sub> Catalyzed by a Chemically Robust Site-Isolated Iron Catalyst. *Angew. Chem., Int. Ed.* **2009**, *48*, 5720–5723.
- (7) White, M. C. Adding Aliphatic C–H Bond Oxidations to Synthesis. *Science* **2012**, *335*, 807–809.
- (8) Garcia-Bosch, I.; Siegler, M. A. Copper-Catalyzed Oxidation of Alkanes with H<sub>2</sub>O<sub>2</sub> under a Fenton-like Regime. *Angew. Chem., Int. Ed.* **2016**, *55*, 12873–12876.
- (9) Rousseau, G.; Breit, B. Removable Directing Groups in Organic Synthesis and Catalysis. *Angew. Chem., Int. Ed.* **2011**, *50*, 2450–2494.
- (10) Trammell, R.; See, Y. Y.; Herrmann, A. T.; Xie, N.; Díaz, D. E.; Siegler, M. A.; Baran, P. S.; Garcia-Bosch, I. Decoding the Mechanism of Intramolecular Cu-Directed Hydroxylation of sp<sup>3</sup> C–H Bonds. *J. Org. Chem.* **2017**, *82*, 7887–7904.
- (11) Schonecker, B.; Zheldakova, T.; Liu, Y.; Kotteritzsch, M.; Gunther, W.; Gørls, H. Biomimetic hydroxylation of nonactivated CH<sub>2</sub> groups with copper complexes and molecular oxygen. *Angew. Chem., Int. Ed.* **2003**, *42*, 3240–3244.
- (12) Schonecker, B.; Zheldakova, T.; Lange, C.; Gunther, W.; Gørls, H.; Bohl, M. Intramolecular gamma-hydroxylations of nonactivated C–H bonds with copper complexes and molecular oxygen. *Chem. - Eur. J.* **2004**, *10*, 6029–6042.
- (13) Schonecker, B.; Lange, C.; Zheldakova, T.; Gunther, W.; Gørls, H.; Vaughan, G. Copper-mediated regio- and stereoselective 12 beta-hydroxylation of steroids with molecular oxygen and an unexpected 12 beta-chlorination. *Tetrahedron* **2005**, *61*, 103–114.
- (14) See, Y. Y.; Herrmann, A. T.; Aihara, Y.; Baran, P. S. Scalable C–H Oxidation with Copper: Synthesis of Polyoxypregnanes. *J. Am. Chem. Soc.* **2015**, *137*, 13776–13779.
- (15) Charest, M. G.; Lerner, C. D.; Brubaker, J. D.; Siegel, D. R.; Myers, A. G. A Convergent Enantioselective Route to Structurally Diverse 6-Deoxytetracycline Antibiotics. *Science* **2005**, *308*, 395–398.
- (16) Miller, J. A. Metal-promoted Fries rearrangement. *J. Org. Chem.* **1987**, *52*, 322–323.
- (17) Choy, P. Y.; Kwong, F. Y. Palladium-Catalyzed ortho-CH-Bond Oxygenation of Aromatic Ketones. *Org. Lett.* **2013**, *15*, 270–273.
- (18) Shan, G.; Yang, X.; Ma, L.; Rao, Y. Pd-Catalyzed C–H Oxygenation with TFA/TFAA: Expedient Access to Oxygen-Containing Heterocycles and Late-Stage Drug Modification. *Angew. Chem., Int. Ed.* **2012**, *51*, 13070–13074.
- (19) Kim, K.; Choe, H.; Jeong, Y.; Lee, J. H.; Hong, S. Ru(II)-Catalyzed Site-Selective Hydroxylation of Flavone and Chromone Derivatives: The Importance of the 5-Hydroxyl Motif for the Inhibition of Aurora Kinases. *Org. Lett.* **2015**, *17*, 2550–2553.
- (20) Tezuka, N.; Shimojo, K.; Hirano, K.; Komagawa, S.; Yoshida, K.; Wang, C.; Miyamoto, K.; Saito, T.; Takita, R.; Uchiyama, M. Direct Hydroxylation and Amination of Arenes via Deprotonative Cupration. *J. Am. Chem. Soc.* **2016**, *138*, 9166–9171.
- (21) Elwell, C. E.; Gagnon, N. L.; Neisen, B. D.; Dhar, D.; Spaeth, A. D.; Yee, G. M.; Tolman, W. B. Copper–Oxygen Complexes Revisited: Structures, Spectroscopy, and Reactivity. *Chem. Rev.* **2017**, *117*, 2059–2107.
- (22) Citek, C.; Herres-Pawlis, S.; Stack, T. D. P. Low Temperature Syntheses and Reactivity of Cu<sub>2</sub>O<sub>2</sub> Active-Site Models. *Acc. Chem. Res.* **2015**, *48*, 2424–2433.
- (23) Trammell, R.; Rajabimoghadam, K.; Garcia-Bosch, I. Copper-Promoted Functionalization of Organic Molecules: from Biologically Relevant Cu/O<sub>2</sub> Model Systems to Organometallic Transformations. *Chem. Rev.* **2019**, *119*, 2954–3031.
- (24) Quist, D. A.; Diaz, D. E.; Liu, J. J.; Karlin, K. D. Activation of dioxygen by copper metalloproteins and insights from model complexes. *JBIC, J. Biol. Inorg. Chem.* **2017**, *22*, 253–288.
- (25) Maiti, D.; Lee, D.-H.; Gaoutchenova, K.; Würtele, C.; Holthausen, M. C.; Narducci Sarjeant, A. A.; Sundermeyer, J.; Schindler, S.; Karlin, K. D. Reactions of a Copper(II) Superoxo Complex Lead to C–H and O–H Substrate Oxygenation: Modeling Copper-Monooxygenase C–H Hydroxylation. *Angew. Chem., Int. Ed.* **2008**, *47*, 82–85.
- (26) Kunishita, A.; Kubo, M.; Sugimoto, H.; Ogura, T.; Sato, K.; Takui, T.; Itoh, S. Mononuclear Copper(II)–Superoxo Complexes that Mimic the Structure and Reactivity of the Active Centers of PHM and DbM. *J. Am. Chem. Soc.* **2009**, *131*, 2788–2789.
- (27) Lee, Y.; Lee, D. H.; Narducci Sarjeant, A. A.; Zakharov, L. N.; Rheingold, A. L.; Karlin, K. D. Thioether Sulfur Oxygenation from O<sub>2</sub> or H<sub>2</sub>O<sub>2</sub> Reactivity of Copper Complexes with Tridentate N<sub>2</sub>S<sub>thioether</sub> Ligands. *Inorg. Chem.* **2006**, *45*, 10098–10107.
- (28) Kim, S.; Ginsbach, J. W.; Lee, J. Y.; Peterson, R. L.; Liu, J. J.; Siegler, M. A.; Sarjeant, A. A.; Solomon, E. I.; Karlin, K. D. Amine Oxidative N-Dealkylation via Cupric Hydroperoxide Cu–OOH Homolytic Cleavage Followed by Site-Specific Fenton Chemistry. *J. Am. Chem. Soc.* **2015**, *137*, 2867–2874.
- (29) Salvador, T. K.; Arnett, C. H.; Kundu, S.; Sapiezynski, N. G.; Bertke, J. A.; Raghbi Boroujeni, M.; Warren, T. H. Copper Catalyzed sp<sup>3</sup> C–H Etherification with Acyl Protected Phenols. *J. Am. Chem. Soc.* **2016**, *138*, 16580–16583.
- (30) Mirica, L. M.; Vance, M.; Rudd, D. J.; Hedman, B.; Hodgson, K. O.; Solomon, E. I.; Stack, T. D. P. Tyrosinase Reactivity in a Model Complex: An Alternative Hydroxylation Mechanism. *Science* **2005**, *308*, 1890–1892.
- (31) Itoh, S.; Kumei, H.; Taki, M.; Nagatomo, S.; Kitagawa, T.; Fukuzumi, S. Oxygenation of phenols to catechols by a (μ-η<sup>2</sup>:η<sup>2</sup>-peroxy)dycopper(II) complex: mechanistic insight into the phenolase activity of tyrosinase. *J. Am. Chem. Soc.* **2001**, *123*, 6708–6709.
- (32) Garcia-Bosch, I.; Company, A.; Frisch, J. R.; Torrent-Sucarrat, M.; Cardellach, M.; Gamba, I.; Güell, M.; Casella, L.; Que, L., Jr;

Ribas, X.; Luis, J. M.; Costas, M. O<sub>2</sub> Activation and Selective Phenolate *ortho* Hydroxylation by an Unsymmetric Dicopper  $\mu$ - $\eta^1$ : $\eta^1$ -Peroxo Complex. *Angew. Chem., Int. Ed.* **2010**, *49*, 2406–2409.

(33) Rolff, M.; Schottenheim, J.; Peters, G.; Tuczek, F. The First Catalytic Tyrosinase Model System Based on a Mononuclear Copper(I) Complex: Kinetics and Mechanism. *Angew. Chem., Int. Ed.* **2010**, *49*, 6438–6442.

(34) Hoffmann, A.; Citek, C.; Binder, S.; Goos, A.; Rübhausen, M.; Troeppner, O.; Ivanović-Burmazović, I.; Wasinger, E. C.; Stack, T. D. P.; Herres-Pawlis, S. Catalytic Phenol Hydroxylation with Dioxxygen: Extension of the Tyrosinase Mechanism beyond the Protein Matrix. *Angew. Chem., Int. Ed.* **2013**, *52*, 5398–5401.

(35) Esguerra, K. V. N.; Fall, Y.; Petitjean, L.; Lumb, J.-P. Controlling the Catalytic Aerobic Oxidation of Phenols. *J. Am. Chem. Soc.* **2014**, *136*, 7662–7668.

(36) Huang, Z.; Lumb, J.-P. A Catalyst-Controlled Aerobic Coupling of *ortho*-Quinones and Phenols Applied to the Synthesis of Aryl Ethers. *Angew. Chem., Int. Ed.* **2016**, *55*, 11543–11547.

(37) Esguerra, K. V. N.; Lumb, J.-P. Selectivity in the Aerobic Dearomatization of Phenols: Total Synthesis of Dehydronornuciferine by Chemo- and Regioselective Oxidation. *Angew. Chem., Int. Ed.* **2018**, *57*, 1514–1518.

(38) Blain, I.; Giorgi, M.; De Raggi, I.; Réglie, M. Substrate-Binding Ligand Approach in Chemical Modeling of Copper-Containing Monooxygenases, I Intramolecular Stereoselective Oxygen Atom Insertion into a Non-Activated C-H Bond. *Eur. J. Inorg. Chem.* **2000**, *2000*, 393–398.

(39) Champloy, F.; Benali-Cherif, N.; Bruno, P.; Blain, I.; Pierrot, M.; Réglie, M.; Michalowicz, A. Studies of Copper Complexes Displaying N3S Coordination as Models for Cu<sub>B</sub> Center of Dopamine  $\beta$ -Hydroxylase and Peptidylglycine  $\alpha$ -Hydroxylating Monooxygenase. *Inorg. Chem.* **1998**, *37*, 3910–3918.

(40) Becker, J.; Gupta, P.; Angersbach, F.; Tuczek, F.; Näther, C.; Holthausen, M. C.; Schindler, S. Selective Aromatic Hydroxylation with Dioxxygen and Simple Copper Imine Complexes. *Chem. - Eur. J.* **2015**, *21*, 11735–11744.

(41) Hamann, J. N.; Rolff, M.; Tuczek, F. Monooxygenation of an appended phenol in a model system of tyrosinase: implications on the enzymatic reaction mechanism. *Dalton Trans.* **2015**, *44*, 3251–3258.

(42) Tsang, A. S. K.; Kapat, A.; Schoenebeck, F. Factors That Control C–C Cleavage versus C–H Bond Hydroxylation in Copper-Catalyzed Oxidations of Ketones with O<sub>2</sub>. *J. Am. Chem. Soc.* **2016**, *138*, 518–526.

(43) Janey, J. M. Recent Advances in Catalytic, Enantioselective  $\alpha$  Aminations and  $\alpha$  Oxygenations of Carbonyl Compounds. *Angew. Chem., Int. Ed.* **2005**, *44*, 4292–4300.

(44) Chaudhari, M. B.; Sutar, Y.; Malpathak, S.; Hazra, A.; Gnanaprakasam, B. Transition-Metal-Free C–H Hydroxylation of Carbonyl Compounds. *Org. Lett.* **2017**, *19*, 3628–3631.

(45) Hassner, A.; Reuss, R. H.; Pinnick, H. W. Synthetic methods. VIII. Hydroxylation of carbonyl compounds via silyl enol ethers. *J. Org. Chem.* **1975**, *40*, 3427–3429.

(46) Kim, S.; Saracini, C.; Siegler, M. A.; Drichko, N.; Karlin, K. D. Coordination Chemistry and Reactivity of a Cupric Hydroperoxide Species Featuring a Proximal H-Bonding Substituent. *Inorg. Chem.* **2012**, *51*, 12603–12605.

(47) Note that a competition experiment was conducted in which an equimolar mixture of **L1** and **L7** was oxidized with 1 equiv of Cu<sup>I</sup> and 5 equiv of H<sub>2</sub>O<sub>2</sub> at –20 °C and quenched after different reaction times, the organic products were analyzed, and the kinetic isotope effect was calculated. The values obtained (between 0.9 and 1.1) are consistent with the KIE calculated in the UV–vis experiments. See the [Supporting Information](#) for further details.

(48) Holland, P. L.; Rodgers, K. R.; Tolman, W. B. Is the Bis(m-oxo)dicopper Core Capable of Hydroxylating an Arene. *Angew. Chem., Int. Ed.* **1999**, *38*, 1139–1142.

(49) Kunishita, A.; Teraoka, J.; Scanlon, J. D.; Matsumoto, T.; Suzuki, M.; Cramer, C. J.; Itoh, S. Aromatic Hydroxylation Reactivity

of a Mononuclear Cu(II)-Alkylperoxo Complex. *J. Am. Chem. Soc.* **2007**, *129*, 7248–7249.

(50) Olah, G. A. Aromatic substitution. XXVIII. Mechanism of electrophilic aromatic substitutions. *Acc. Chem. Res.* **1971**, *4*, 240–248.

(51) Vilella, L.; Conde, A.; Balcells, D.; Diaz-Requejo, M. M.; Lledos, A.; Perez, P. J. A competing, dual mechanism for catalytic direct benzene hydroxylation from combined experimental-DFT studies. *Chem. Sci.* **2017**, *8*, 8373–8383.

(52) Mirica, L. M.; Ottenwaelder, X.; Stack, T. D. P. Structure and Spectroscopy of Copper-Dioxxygen Complexes. *Chem. Rev.* **2004**, *104*, 1013–1045.

(53) Paul, P. P.; Tyeklár, Z.; Jacobson, R. R.; Karlin, K. D. Reactivity Patterns and Comparisons in Three Classes of Synthetic Copper-Dioxxygen {Cu<sub>2</sub>O<sub>2</sub>} Complexes: Implication for Structure and Biological Relevance. *J. Am. Chem. Soc.* **1991**, *113*, 5322–5332.

(54) Lewis, E. A.; Tolman, W. B. Reactivity of Dioxxygen-Copper Systems. *Chem. Rev.* **2004**, *104*, 1047–1076.

(55) Maiti, D.; Fry, H. C.; Woertink, J. S.; Vance, M. A.; Solomon, E. I.; Karlin, K. D. A 1:1 Copper-Dioxxygen Adduct is an End-on Bound Superoxo Copper(II) Complex which Undergoes Oxygenation Reactions with Phenols. *J. Am. Chem. Soc.* **2007**, *129*, 264–265.

(56) Schatz, M.; Raab, V.; Foxon, S. P.; Brehm, G.; Schneider, S.; Reiher, M.; Holthausen, M. C.; Sundermeyer, J.; Schindler, S. Combined spectroscopic and theoretical evidence for a persistent end-on copper superoxo complex. *Angew. Chem., Int. Ed.* **2004**, *43*, 4360–4363.

(57) Würtele, C.; Gaoutchenova, E.; Harms, K.; Holthausen, M. C.; Sundermeyer, J.; Schindler, S. Crystallographic Characterization of a Synthetic 1:1 End-On Copper Dioxxygen Adduct Complex. *Angew. Chem., Int. Ed.* **2006**, *45*, 3867–3869.

(58) Peterson, R. L.; Himes, R. A.; Kotani, H.; Suenobu, T.; Tian, L.; Siegler, M. A.; Solomon, E. I.; Fukuzumi, S.; Karlin, K. D. Cupric Superoxo-Mediated Intermolecular C–H Activation Chemistry. *J. Am. Chem. Soc.* **2011**, *133*, 1702–1705.

(59) Maiti, D.; Lucas, H. R.; Sarjeant, A. A. N.; Karlin, K. D. Aryl Hydroxylation from a Mononuclear Copper-Hydroperoxo Species. *J. Am. Chem. Soc.* **2007**, *129*, 6998–6999.

(60) Kunishita, A.; Ertem, M. Z.; Okubo, Y.; Tano, T.; Sugimoto, H.; Ohkubo, K.; Fujieda, N.; Fukuzumi, S.; Cramer, C. J.; Itoh, S. Active Site Models for the CuA Site of Peptidylglycine  $\alpha$ -Hydroxylating Monooxygenase and Dopamine  $\beta$ -Monooxygenase. *Inorg. Chem.* **2012**, *51*, 9465–9480.

(61) Becker, J.; Zhyhadlo, Y. Y.; Butova, E. D.; Fokin, A. A.; Schreiner, P. R.; Förster, M.; Holthausen, M. C.; Specht, P.; Schindler, S. Aerobic Aliphatic Hydroxylation Reactions by Copper Complexes: A Simple Clip-and-Cleave Concept. *Chem. - Eur. J.* **2018**, *24*, 15543–15549.

(62) Tsuji, T.; Zaoputra, A. A.; Hitomi, Y.; Mieda, K.; Ogura, T.; Shiota, Y.; Yoshizawa, K.; Sato, H.; Kodera, M. Specific Enhancement of Catalytic Activity by a Dicopper Core: Selective Hydroxylation of Benzene to Phenol with Hydrogen Peroxide. *Angew. Chem., Int. Ed.* **2017**, *56*, 7779–7782.

(63) Ciano, L.; Davies, G. J.; Tolman, W. B.; Walton, P. H. Bracing copper for the catalytic oxidation of C–H bonds. *Nat. Catal.* **2018**, *1*, 571–577.